Infection, Genetics and Evolution 75 (2019) 103985

Contents lists available at ScienceDirect

Infection, Genetics and Evolution

journal homepage: www.elsevier.com/locate/meegid

Short communication

High-throughput identification of microRNAs in *Taenia hydatigena*, a cestode threatening livestock breeding industry

Jin'en Wu[a], Jing Yang[a], Guitian He[a], Xiaola Guo[a], Ivan Kutyrev[b], Omnia M. Kandil[c], Yadong Zheng[a,d,*]

[a] *State Key Laboratory of Veterinary Etiological Biology, Key Laboratory of Veterinary Parasitology of Gansu Province, Lanzhou Veterinary Research Institute, CAAS, Lanzhou 730046, China*
[b] *Institute of General and Experimental Biology, Siberian Branch of Russian Academy of Sciences, Sakhyanovoi st. 6, 670047 Ulan-Ude, Russia*
[c] *Depterment of Parasitology and Animal Disease, Veterinary Research Division, National Research Centre, Giza 12622, Egypt*
[d] *Jiangsu Co-innovation Center for Prevention and Control of Important Animal Infectious Diseases and Zoonoses, Yangzhou 225009, China*

ARTICLE INFO

Keywords:
Taenia hydatigena
miRNA
Cestode

ABSTRACT

Infection of *Cysticercus tenuicollis*, the larval stage of *Taenia hydatigena*, is extensively found in sheep and pigs and jeopardizes the breeding and meat industry. miRNAs are a subclass of small noncoding regulatory RNAs and closely associated with the pathogenesis and biology of parasites. Here, using HiSeq sequencing we identified 49 known and 2 potential novel miRNAs in *C. tenuicollis*, of which both thy-miR-71 and -87 were predominant. Using RT-qPCR, 6 selected miRNAs were validated, and thy-miR-71 and -miR-87 were confirmed to be highly expressed, with the copy number of approximately 82,340 ± 2079 and 19,580 ± 609 per 1 ng total RNA, respectively. Similar to other cestodes, *T. hydatigena* was predicted to have two conserved miRNA clusters thy-miR-71/2c/2b and thy-miR-4989/277, and three members of the former were confirmed to reside sequentially within the genomic region of 253 bp by PCR. The current data provide us a valuable resource for further studies of a role of miRNAs in *T. hydatigena* biology and infection.

1. Introduction

Cysticercus tenuicollis is the metacestode of *Taenia hydatigena* that belongs to class Cestoidea of the Platyhelminthes. The development of *T. hydatigena* requires two distinct hosts to complete its life cycle: pigs, sheep and goats sever as an intermediate host, while dogs and other canines as a definitive host. *C. tenuicollis* mainly parasitizes on the liver serosa, omentum, mesentery and peritoneum of intermediate hosts (Braae et al., 2015; Singh et al., 2015; Sissay et al., 2008), leading to tissue damage and even death (Luo et al., 2017). Therefore, the disease by *C. tenuicollis* poses a threat to the livestock breeding and meat production industry.

microRNAs (miRNAs) are a class of endogenous and single-stranded RNA with a size of 18–22 nt, being involved in various physiological and pathological processes via regulating translational repression or mRNA degradation in many organisms (Wu et al., 2018). In recent years, a large number of studies have demonstrated that miRNAs play a major role in parasite growth and development, and host and parasite interactions (Arora et al., 2017; Cai et al., 2016; Entwistle and Wilson, 2017; Zheng et al., 2013). At present, *T. hydatigena* miRNA profiles remain unknown.

Using deep sequencing technology and RT-qPCR, we herein investigated the genome-wide expression profile of miRNAs, which provides rich data for further studies of their roles in *T. hydatigena* biology and infection.

2. Materials and methods

2.1. Ethical statement

The study was assessed and approved by Ethics Committee of Lanzhou Veterinary Research Institute, CAAS. All animal experiments were performed strictly according to the Animal Ethics Procedures and Guidelines of the People's Republic of China.

2.2. Isolation of *C. tenuicollis* and total RNA extraction

Fresh *C. tenuicollis* samples were carefully collected from the liver of naturally-infected adult sheep and immediately washed with sterile and ice-cold PBS. Subsequently, 50 mg of parasite mass were promptly used

---

[*] Corresponding author at: 1 Xujiaping, Yanchangbu, Lanzhou 730046, Gansu, China.
E-mail address: zhengyadong@caas.cn (Y. Zheng).

https://doi.org/10.1016/j.meegid.2019.103985
Received 24 April 2019; Received in revised form 23 July 2019; Accepted 26 July 2019
Available online 27 July 2019
1567-1348/ © 2019 Elsevier B.V. All rights reserved.

for total RNA extraction according to the instructions of TRIzol LS Reagent (Invitrogen) with some modifications. Briefly, parasite mass was ground into powder with a mortar in liquid nitrogen. After addition of 10 μg of glycogen (10 mg/mL, Invitrogen), RNA-containing aqueous supernatant was incubated at −20 °C overnight, and RNA pellets were air-dried for 5 min and then dissolved in 40 μL of RNase-free water. The concentration and integrality of the isolated RNA were examined using Agilent Bioanalyzer (Agilent). Afterwards, total RNA samples were immediately used or stored at −80 °C until further use.

2.3. *High-throughput sequencing and data analysis*

Small RNA sequencing was carried out using Hiseq (BGI) as follows. Briefly, the small RNA fragments with sizes between 18 and 30 nt were isolated and purified using a PAGE gel. Purified small RNA was ligated with 3′ and 5′ adaptors, and then RT-PCR enrichment was performed by ABI StepOnePlus Real-Time PCR System. The PCR products were purified using 10% PAGE and used for deep sequencing.

To obtain clean reads, the reads with poly A, shorter than 18 nt, and without the insert tags were removed from raw data. Meanwhile, the reads derived from tRNA, rRNA, snoRNA and snRNA, repetitive sequences and small degraded mRNA were also removed. Due to the lack of *T. hydatigena* genome data, the clean reads were mapped to the *Taenia solium* genome (https://parasite.wormbase.org/Taenia_solium_prjna170813/Info/Index/) by SOAP2 software to analyze their location and distribution on the genome as previously described (Li et al., 2009; Zheng, 2017). For the prediction of novel miRNAs, miRDeep2 algorithm and miReap program (http://sourceforge.net/projects/mireap/) were used as previously reported (Friedlander et al., 2008). RNAfolder was used to analyze the secondary structure of the thy-miR-71/2c/2c cluster (http://rna.tbi.univie.ac.at/cgi-bin/RNAWebSuite/RNAfold.cgi).

2.4. *DNA extraction and PCR amplification of the thy-miR-71/2c/2b cluster*

Approximately 50 mg of *C. tenuicollis* tissues were used for the isolation of genomic DNA by Tissue DNA Kit (Omega Bio-Tek) according to the manufacturer's instructions. In brief, fresh *C. tenuicollis* tissues were ground into powder in liquid nitrogen. Extracted DNA was eluted in 100 μL of elution buffer and then immediately used for PCR amplification or stored at −80 °C until further use. Using specific primers (Table 1), the thy-miR-71/2c/2b cluster was amplified by PCR using 2 × Premix Taq™ (TaKaRa) with the following steps: denaturation at 98 °C for 5 min, followed by 35 cycles of 98 °C for 30 s and 60 °C for 1 min. A PCR product was resolved on 1.2% agarose gel, purified and sequenced (Tianqi).

Table 1
The primers used in this study.

Primer	Sequence (5′-3′)
RT primer	GCGAGCACAGAATTAATACGACTCACTATAGG$(T)_{12}$VN[a]
universal reverse primer	GCGAGCACAGAATTAATACGAC
thy-miR-190-5p	GAGATATGTTTGGGTTACTTG
thy-miR-71	CGTGAAAGACGATGGTAGTGAG
thy-miR-61-3p	TGACTAGAAAGAGCACTCAC
thy-let-7-5p	GCTGAGGTAGTGTTTCGAATGTCT
thy-miR-87	GTCGTGAGCAAAGTTTCAGGTGT
thy-novel-miR2	GATTGCACTACCTATCGCCCATA
miR-71/2c/2b cluster-F	GCAGTCATCTCATGAAAGACG
miR-71/2c/2b cluster-R	TCCCAAGCAGGGCTGTGATAC

[a] ‘V' stands for A, G or C; ‘N' stands for A, T, G or C.

2.5. *Construction of recombinant plasmid*

Using the RT primer (Table 1), first-strand cDNA of miRNAs was synthesized using 2 μg of total RNA by All-in-one miRNA First-strand cDNA Synthesis Kit (GeneCopoeia) according to the manufacturer's protocols. PCR reactions were performed using 2 × Premix Taq™ (TaKaRa) with the universal reverse primer and the primer specific for individual miRNAs (Table 1) according to the following procedures: denaturation at 98 °C for 5 min, followed by 35 cycles of 98 °C for 30 s and 68 °C for 60 s. PCR products were analyzed using 2% agarose gel electrophoresis and purified. In controls, cDNA was replaced by water or reverse transcriptase-absent cDNA in PCR reaction preparations.

For plasmid construction, purified PCR products were cloned into *pEASY*®-T5 Zero Cloning Vector using *pEASY*®-T5 Zero Cloning Kit (TransGen Biotech) and transformed into *Trans1*-T1 competent cells (TransGen Biotech) according to the manufacturer's instructions. Approximately 150 μL of transformed competent cells were spread onto LB agar medium containing 100 μg/mL of ampicillin. The positive clones were picked and cultured overnight in LB medium containing ampicillin. The recombinant plasmids were extracted using MiniBEST Plasmid Purification Kit (TaKaRa) and sequenced (Tianqi).

2.6. *Standard curves and absolute quantification qPCR analysis*

To verify the reliability of sequencing data, 5 known and 1 novel miRNAs were selected for RT-qPCR analysis (Table 1). The concentration of recombinant plasmids was measured using Nanodrop (ThermoFisher Scientific), and the corresponding copy number was determined by the following formula as reported elsewhere (Kang et al., 2018; Whelan et al., 2003).

$$\text{DNA (copy number)} = \frac{6.02 \times 10^{23}(\text{copy/mol}) \times \text{DNA amount(g)}}{\text{DNA length(dp)} \times 660(\text{g/mol/dp})}$$

10-fold serial dilutions (1×10^{10} to 1×10^{2} copies/μL) of recombinant plasmids were used to construct individual standard curves and each dilution was repeated 3 times. After reverse transcription, cDNA products of those 6 miRNAs were diluted 6.6 times with sterile H_2O. Real-time qPCR was performed with ABI 7500 Thermal Cycler (ThermoFisher Scientific) using All-in-one qPCR Mix Kit (GeneCopoeia) with the following protocol: denaturation at 95 °C for 5 min, followed by 40 cycles of 95 °C for 15 s and 60 °C for 1 min. PCR products were resolved using 10% DNA PAGE gel as previously reported (Cai et al., 2015). The absolute expression level of every selected miRNA was calculated using the following equation as previously reported (Formisano-Treziny et al., 2012):

$$\text{Ct} = \text{slope} \times \log(\text{copy number}) + \text{intercept}.$$

3. Results and discussion

3.1. *An overview of the deep sequencing data*

After removal of adaptors, contaminants and low-quality reads, a total of 19,400,954 clean reads were obtained from the small RNA sequencing library (the raw data was deposited in NCBI with the accession number of SUB5749635). Of them, approximately 60% (11,692,579) of clean reads were mapped to the *T. solium* genome, 43.81% of which were annotated as miRNAs. All the mapped reads have been cataloged, including miRNAs, rRNAs, tRNAs, snRNAs and snoRNAs (Fig. 1A). For the size distribution of miRNAs, it was found that the majority of miRNAs were 22 nt in length (Fig. 1B and Table 2), which is consistent with the previous results reported in other cestode species (Cucher et al., 2015; Guo and Zheng, 2018; Zheng, 2017).

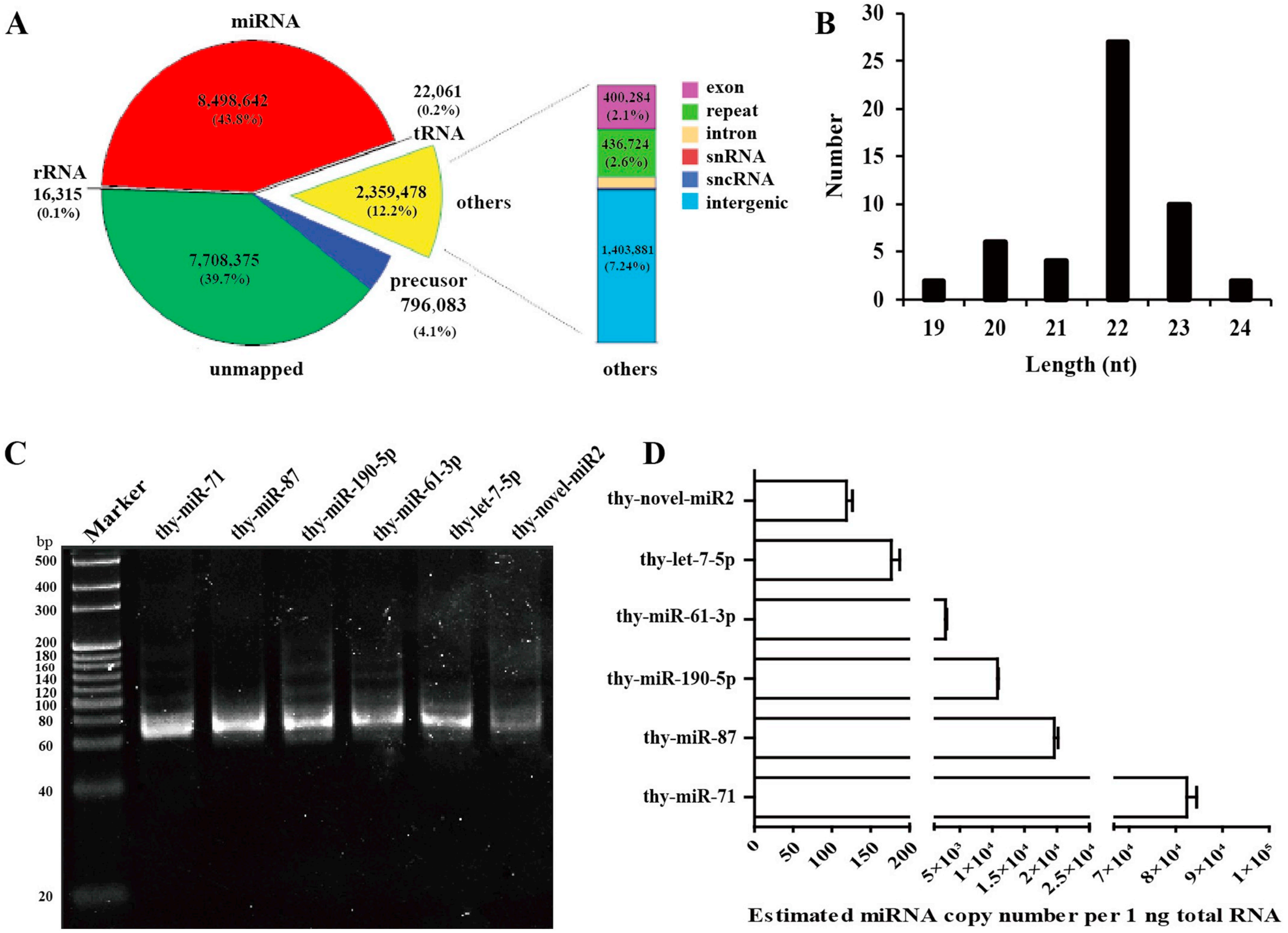

Fig. 1. Identification of *T. hydatigena* miRNAs All the mapped clean reads were annotated, including miRNAs, rRNAs, tRNAs, snRNAs and snoRNAs (A). The length distribution of identified miRNAs (B). Using PCR, 6 selected miRNAs including thy-miR-71 (lane 1), −miR-87 (lane 2), −190-5p (lane 3), −61-3p (lane 4), −let-7-5p (lane 5) and -novel-miR2 (lane 6) were amplified with high specificity. 20 bp DNA ladder (Dye Plus) markers (Takara) were shown on the left (C). Moreover, the copy number of 6 selected miRNAs in 1 ng total RNA was estimated (D).

3.2. Identification and characterization of miRNAs

A total of 49 known and 2 novel miRNAs were identified in *C. tenuicollis*, and these known miRNAs belonged to 27 different miRNA families (Table 2 and Fig. A2). By comparison of the abundance of miRNAs identified, it was found that thy-miR-71 was absolutely predominant with nearly 32.6% (2,769,280/8,498,642) of total miRNA reads, followed by thy-miR-87 (17.1%) and -let-7-5p (9.0%). However, some miRNAs was lowly expressed, such as thy-miR-124b-5p, − 219-3p and − 31-3p with < 10 reads (Table 2). These results indicate that *T. hydatigena* miRNAs have a broad range in expression, which may be closely related to the different functions of distinct miRNAs.

Both the precursors of 2 novel miRNAs, thy-novel-miR1 and -miR2, were predicted to have a typical secondary structure with a potential hairpin loop and 3′-overhangs (Fig. A2). Moreover, thy-novel-miR2 was further verified to lowly express in *C. tenuicollis* (Fig. 1C and D), suggesting an authentic miRNA. At present, the *Taenia hydatigena* genome is not available and the use of *T. solium* genome for read mapping inevitably introduces artifacts in identification of known and novel miRNAs. Therefore, reanalysis is necessary if the *Taenia hydatigena* genome will be deciphered in future.

Among the identified miRNAs, thy-miR-71 and -4989-3p clustered together with thy-miR-2c/2b and -277a-3p, respectively. Moreover, sequence analysis confirmed that the thy-miR-71/2c/2b cluster was conserved and predicted to form stable secondary structure, consisting of thy-miR-71, − 2c and -2b that sequentially reside within the genomic region of 253 bp (Fig. A1). It is worth noting that miRNAs in these two clusters seem to be differentially expressed (Table 2). In general, miRNAs in the same cluster are co-transcribed into a single pre-miRNA, which is then cleaved into mature miRNAs (Bartel, 2004). However, it is still puzzling that these mature miRNAs from the same cluster have different abundance. This characteristic was also reported in other cestodes, such as *Taenia ovis*, *Hydatigera taeniaeformis*, *Taenia asiatica*, and *Echinococcus* spp. (Guo and Zheng, 2018; Zheng, 2017). It may suggest that some specific miRNAs can be preferentially cleaved due to their important functions (Cucher et al., 2015). miR-71 is highly expressed in almost all worms (Ai et al., 2012; Cucher et al., 2015; Guo and Zheng, 2018). Many studies have reported that miR-71 not only regulates the development and longevity of helminths (Boulias and Horvitz, 2012; Cucher et al., 2015; Guo et al., 2017), but also plays essential roles in parasite infection and interactions with the host (Zheng et al., 2013; Zheng et al., 2016). Consistently, it was recently reported that parasite-derived miR-71 was detected in the blood and lymph of hosts infected by some parasites (Zheng, 2017; Zheng et al., 2016). Of high interest is to investigate the roles of thy-miR-71 in *T. hydatigena* development and infection in future studies.

Table 2
The known and novel miRNAs identified in *T. hydatigena.*

miRNA	Sequence (5′- 3′)	Location (5′- 3′)	Length (nt)	Read count	Family
thy-miR-71	UGAAAGACGAUGGUAGUGAGA	Tsm_contig_01703: 2152–2173/+	21	2,769,280	miR-71
thy-miR-87	GUGAGCAAAGUUUCAGGUGUGC	Tsm_contig_00046: 21990–22,012/+	22	1,450,427	miR-87
thy-let-7-5p	UGAGGUAGUGUUUCGAAUGUCU	Tsm_contig_01305: 3818–3840/−	22	767,733	let-7
thy-miR-277a-3p	UAAAUGCAUUUUCUGGCCCGUA	Tsm_contig_00002: 355714–355,736/+	22	490,600	miR-277
thy-miR-2c-3p	UCACAGCCAAUAUUGAUGAA	Tsm_contig_01703: 2286–2306/+	20	378,249	miR-2
thy-miR-190-5p	AGAUAUGUUUGGGUUACUUGGUG	Tsm_contig_00076: 133403–133,426/−	23	358,409	miR-190
thy-miR-4989-3p	AAAAUGCACCAACUAUCUGAGA	Tsm_contig_00002: 355581–355,603/+	22	326,575	miR-277
thy-miR-1-5p	UGGAAUGUUGUGAAGUAUGU	Tsm_contig_00015: 112264–112,284/+	20	326,357	miR-1
thy-miR-125-5p	UCCCUGAGACCCUAGAGUUGUC	Tsm_contig_00925: 18221–18,243/−	22	311,055	miR-125
thy-miR-281-3p	UGUCAUGGAGUUGCUCUCUAUA	Tsm_contig_00278: 50132–50,154/+	22	285,472	miR-281
thy-miR-10a-5p	CACCCUGUAGACCCGAGUUUGA	Tsm_contig_00001: 733585–733,607/−	22	146,804	miR-10
thy-miR-9-5p	UCUUUGGUUAUCUAGCUGUGUG	Tsm_contig_00972: 16152–16,174/−	22	140,115	miR-9
thy-miR-3479a-3p	UAUUGCACGUUCUUUCGCCAUC	Tsm_contig_00022: 149861–149,883/−	22	119,670	miR-3479
thy-miR-61-3p	UGACUAGAAAGAGCACUCACAUC	Tsm_contig_00547: 54161–54,184/+	23	102,845	miR-61
thy-miR-745-3p	UGCUGCCUGGUAAGAGCUGUGA	Tsm_contig_00001: 902–924/+	22	100,272	miR-745
thy-miR-2b-3p	UAUCACAGCCCUGCUUGGGACACA	Tsm_contig_01703: 2388–2412/+	24	81,157	miR-2
thy-bantam-3p	UGAGAUCGCGAUUACAGCUGAU	Tsm_contig_00288: 81898–81,920/−	22	54,579	bantam
thy-miR-2a-3p	AAUCACAGCCCUGCUUGGAACC	Tsm_contig_00316: 47939–47,961/+	22	50,199	miR-2
thy-miR-219-5p	UGAUUGUCCAUUCGCAUUUCUU	Tsm_contig_03098: 2170–2192/−	22	48,899	miR-219
thy-miR-184-3p	GGGACGGAAGUCUGAAAGGUUU	Tsm_contig_00173: 108768–108,790/+	22	44,235	miR-184
thy-miR-7b-5p	UGGAAGACUUGUGAUUAGAUUGUU	Tsm_contig_00022: 155589–155,613/+	24	36,888	miR-7
thy-miR-124a-3p	UAAGGCACGCGGUGAAUGCCA	Tsm_contig_02167: 4346–4366/+	21	20,680	miR-124
thy-miR-61–5p	CGUGAGGCCCUUUCUUGUGCAUG	Tsm_contig_00547: 54108–54,131/+	23	17,535	miR-61
thy-miR-7-5p	UGGAAGACUGGUGAUAUGUUGU	Tsm_contig_00222: 106111–106,133/−	22	16,111	miR-7
thy-miR-277b-3p	UAAAUGCAAAAUAUCUGGUUAUG	Tsm_contig_00080: 97038–97,061/−	23	12,355	miR-277
thy-miR-2162-3p	UAUUAUGCAACUUUUCACUCC	Tsm_contig_00907: 20879–20,900/+	21	10,986	miR-2162
thy-miR-190-3p	CCAGUGACCAAACAUAUUC	Tsm_contig_00076: 133364–133,383/−	19	5569	miR-190
thy-miR-124b-3p	UAAGGCACGCGGUGAAUACC	Tsm_contig_00021: 132918–132,938/−	20	5554	miR-124
thy-miR-96-5p	AUUGGCACUUUUGGAAUUGUC	Tsm_contig_00412: 68636–68,657/+	21	3618	miR-96
thy-miR-153-3p	UUGCAUAGUCUCAUAAGUGCCA	Tsm_contig_00050: 147636–147,658/−	22	2861	miR-153
thy-miR-133-3p	UUGGUCCCCAUUAACCAGCCGC	Tsm_contig_00015: 123944–123,966/+	22	2109	miR-133
thy-miR-4989-5p	UGGGUAGUCGUUGCAUUUCC	Tsm_contig_00002: 355528–355,548/+	20	2085	miR-277
thy-miR-10,293-3p	UAAUUCGAGUCAACAGGGUCGUU	Tsm_contig_00406: 472–495/−	23	1991	miR-10,293
thy-miR-9-3p	CAAGGCUAGAUUUCCAAACAAA	Tsm_contig_00972: 16100–16,122/−	22	1943	miR-9
thy-let-7-3p	ACAUCCGUUUCACUAUCUGCAUA	Tsm_contig_01305: 3783–3806/−	23	1386	let-7
thy-miR-2c-5p	UCGUCAACAUUGCCUGUAGACA	Tsm_contig_01703: 2252–2274/+	22	1253	miR-2
thy-bantam-5p	CGGCUUUUCUCGCGUUCUGAGA	Tsm_contig_00288: 81944–81,966/−	22	775	bantam
thy-miR-125-3p	CAACUCUAAUGUCCCGGGUUAU	Tsm_contig_00587: 14172–14,194/+	22	645	miR-125
thy-miR-3479a-5p	CGGUGAAAGUUUAUGCAUUUACA	Tsm_contig_00022: 149893–149,916/−	23	423	miR-3479
thy-miR-307-3p	UCACAACCUACUUGAUUGAGGGG	Tsm_contig_02301: 4350–4373/−	23	346	miR-307
thy-miR-31–5p	UGGCAAGAUACUGGCGAAGCUGA	Tsm_contig_00183: 113814–113,837/−	23	114	miR-31
thy-miR-36a-3p	UCACCGGGUAGACAUUCCUUGC	Tsm_contig_00495: 44929–44,951/−	22	101	miR-36
thy-miR-36b-3p	UCACCGGGUAGUUAUUACGCCU	Tsm_contig_00086: 22153–22,175/−	22	78	miR-36
thy-miR-96-3p	GACGGUCUAAAAGUGCCGAACA	Tsm_contig_00412: 68711–68,733/+	22	50	miR-96
thy-miR-2d-3p	UACAGGCAAUGUUGACGACG	Tsm_contig_01703: 2250–2270/−	20	22	miR-2
thy-miR-133-5p	GGCUGAUUUGUGGGGCUCAGAA	Tsm_contig_00015: 123903–123,925/+	22	10	miR-133
thy-miR-124b-5p	CAUUCACCGCGUGCCUUAA	Tsm_contig_02167: 4345–4364/−	19	6	miR-124
thy-miR-219-3p	AGAUGUGUGUAUGGGCAUCGCA	Tsm_contig_03098: 2117–2139/−	22	2	miR-219
thy-miR-31-3p	AGCUUCGUCUGGUCUUGCUGCA	Tsm_contig_00183: 113776–113,798/−	22	2	miR-31
thy-novel-miR1	GCCTCGAGGATTGGCCCATT	Tsm_contig_02881: 342–384/−	20	67	unknown
thy-novel-miR2	GATTGCACTACCTATCGCCCATA	Tsm_contig_01679: 2083–2152/−	23	51,410	unknown

3.3. Abundance of selected miRNAs

Using 6 different recombinant plasmids as a template, the standard curves of individual qPCR reactions were constructed and all standard curves' correlation coefficients were in an acceptable range ($R^2 > 0.99$), which indicated a good linearity (Fig. A3). Moreover, all the primers for 6 selected miRNAs were of high specificity, with a single specific product being amplified (Fig. 1C), and no bands were observed in controls (data not shown). Consistent with the sequencing data (Table 2), the thy-miR-71 expression was the highest among the 6 selected miRNAs, with an estimated copy number of 82,340 ± 2079 per 1 ng total RNA, followed by thy-miR-87 (19,580 ± 609), −190-5p (10,800 ± 143), and − 61-3p (2740 ± 92) (Fig. 1D). However, thy-let-7-5p and -novel-miR2 were estimated to have a low copy number of 176 ± 10 and 118 ± 8, respectively, which is not well in agreement with the sequencing data. It is still unclear why this discrepancy occurs. It may be a bias introduced by the PCR enrichment step during small RNA library construction.

4. Conclusions

In the present study, the genome-wide expression of miRNAs in *C. tenuicollis* was defined, which will provide valuable references and help us better understand the roles of miRNAs in the parasite biology and infection.

Declaration of Competing Interest

The authors declare no conflicts of interest.

Acknowledgement

This work was financially supported by the National Natural Science Foundation of China (U1703104 and 31472185) and the National Key Basic Research Program (973 program) of China (2015CB150300).

Appendix A. Appendix

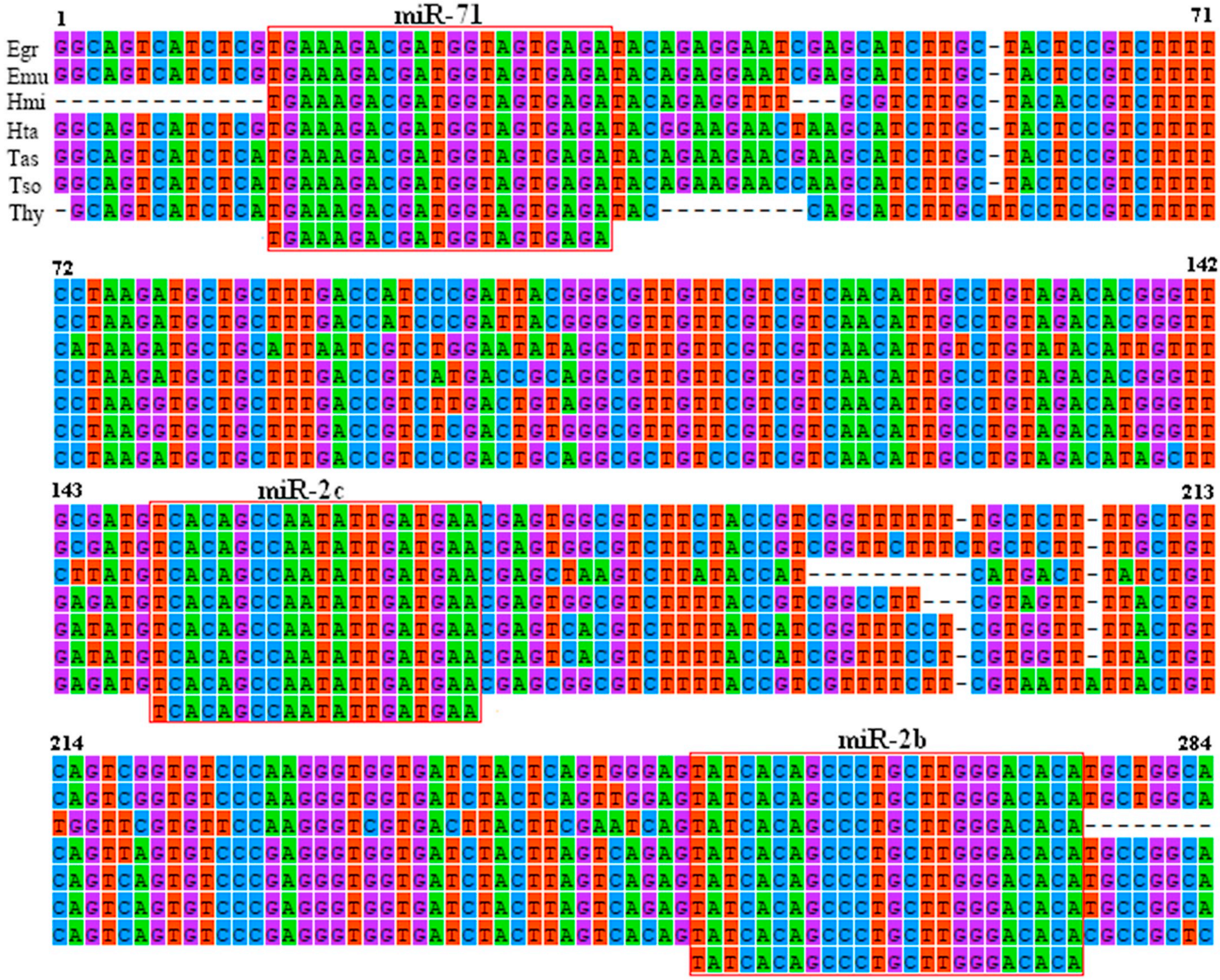

```
    1                 miR-71                                            71
Egr GGCAGTCATCTCGTGAAAGACGATGGTAGTGAGATACAGAGGAATCGAGCATCTTGC-TACTCCGTCTTTT
Emu GGCAGTCATCTCGTGAAAGACGATGGTAGTGAGATACAGAGGAATCGAGCATCTTGC-TACTCCGTCTTTT
Hmi -------------TGAAAGACGATGGTAGTGAGATACAGAGGTTT---GCGTCTTGC-TACACCGTCTTTT
Hta GGCAGTCATCTCGTGAAAGACGATGGTAGTGAGATACGGAAGAACTAAGCATCTTGC-TACTCCGTCTTTT
Tas GGCAGTCATCTCATGAAAGACGATGGTAGTGAGATACAGAAGAACGAAGCATCTTGC-TACTCCGTCTTTT
Tso GGCAGTCATCTCATGAAAGACGATGGTAGTGAGATACAGAAGAACCAAGCATCTTGC-TACTCCGTCTTTT
Thy -GCAGTCATCTCATGAAAGACGATGGTAGTGAGATAC---------CAGCATCTTGCTTCCTCCGTCTTTT
                 TGAAAGACGATGGTAGTGAGA

    72                                                                 142
    CCTAAGATGCTGCTTTGACCATCCCGATTACGGGCGTTGTTCGTCGTCAACATTGCCTGTAGACACGGGTT
    CCTAAGATGCTGCTTTGACCATCCCGATTACGGGCGTTGTTCGTCGTCAACATTGCCTGTAGACACGGGTT
    CATAAGATGCTGCATTAATCGTCTGGAATATAGGCTTTGTTCGTCGTCAACATTGTCTGTATACATTGTTT
    CCTAAGATGCTGCTTTGACCGTCATGACCGCAGGCGTTGTTCGTCGTCAACATTGCCTGTAGACACGGGTT
    CCTAAGGTGCTGCTTTGACCGTCTTGACTGTAGGCGTTGTTCGTCGTCAACATTGCCTGTAGACATGGGTT
    CCTAAGGTGCTGCTTTGACCGTCTCGACTGTGGGCGTTGTTCGTCGTCAACATTGCCTGTAGACATGGGTT
    CCTAAGATGCTGCTTTGACCGTCCCGACTGCAGGCGCTGTCCGTCGTCAACATTGCCTGTAGACATAGCTT

    143           miR-2c                                                 213
    GCGATGTCACAGCCAATATTGATGAACGAGTGGCGTCTTCTACCGTCGGTTTTTT-TGCTCTT-TTGCTGT
    GCGATGTCACAGCCAATATTGATGAACGAGTGGCGTCTTCTACCGTCGGTTCTTTCTGCTCTT-TTGCTGT
    CTTATGTCACAGCCAATATTGATGAACGAGCTAAGTCTTATACCAT----------CATGACT-TATCTGT
    GAGATGTCACAGCCAATATTGATGAACGAGTGGCGTCTTTTACCGTCGGCCTT---CGTAGTT-TTACTGT
    GATATGTCACAGCCAATATTGATGAACGAGTCACGTCTTTTATCATCGGTTTCCT-CGTGGTT-TTACTGT
    GATATGTCACAGCCAATATTGATGAACGAGTCACGTCTTTTACCATCGGTTTCCT-CGTGGTT-TTACTGT
    GAGATGTCACAGCCAATATTGATGAACGAGCGGCGTCTTTTACCGTCGTTTTCTT-CGTAATTATTACTGT
          TCACAGCCAATATTGATGAA

    214                                             miR-2b               284
    CAGTCGGTGTCCCAAGGGTGGTGATCTACTCAGTGGGAGTATCACAGCCCTGCTTGGGACACATGCTGGCA
    CAGTCGGTGTCCCAAGGGTGGTGATCTACTCAGTTGGAGTATCACAGCCCTGCTTGGGACACATGCTGGCA
    TGGTTCGTGTTCCAAGGGTCGTGACTTACTTCGAATCAGTATCACAGCCCTGCTTGGGACACA--------
    CAGTTAGTGTCCCGAGGGTGGTGATCTACTTAGTCAGAGTATCACAGCCCTGCTTGGGACACATGCCGGCA
    CAGTCAGTGTCCCGAGGGTGGTGATCTACTTAGTCAGAGTATCACAGCCCTGCTTGGGACACATGCCGGCA
    CAGTCAGTGTCCCGAGGGTGGTGATCTACTTAGTCAGAGTATCACAGCCCTGCTTGGGACACATGCCGGCA
    CAGTCAGTGTCCCGAGGGTGGTGATCTACTTAGTCACAGTATCACAGCCCTGCTTGGGACACACGCCGCTC
                                           TATCACAGCCCTGCTTGGGACACA
```

Fig. A1. Alignment of miR-71/2c/2b clusters in cestodes (A) The DNA sequences containing miR-71, −2c and -2b from 7 cestodes, including *Echinococcus granulosus* (Egr), *Echinococcus multilocularis* (Emu), *Hymenolepis microstoma* (Hmi), *Hydatigera taeniaeformis* (Hta), *Taenia solium* (Tso), *Taenia asiatica* (Tas) and *Taenia hydatigena* (Thy), were aligned using Clustal Omega with default parameters. Three members in the cluster were boxed and the length was indicated above the aligned sequences. Gaps were filled with '-'. (B) The secondary structure of the thy-miR-71/2c/2b cluster-containing sequence was predicted using RNAfolder.

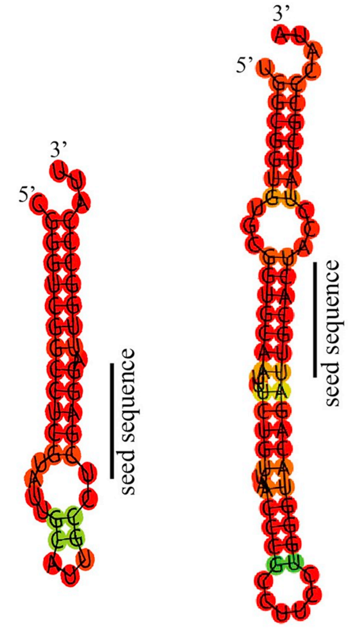

thy-novel-miR1 **thy-novel-miR2**

Fig. A2. The predicted secondary structure of thy-novel-miR1 and thy-novel-miR2.

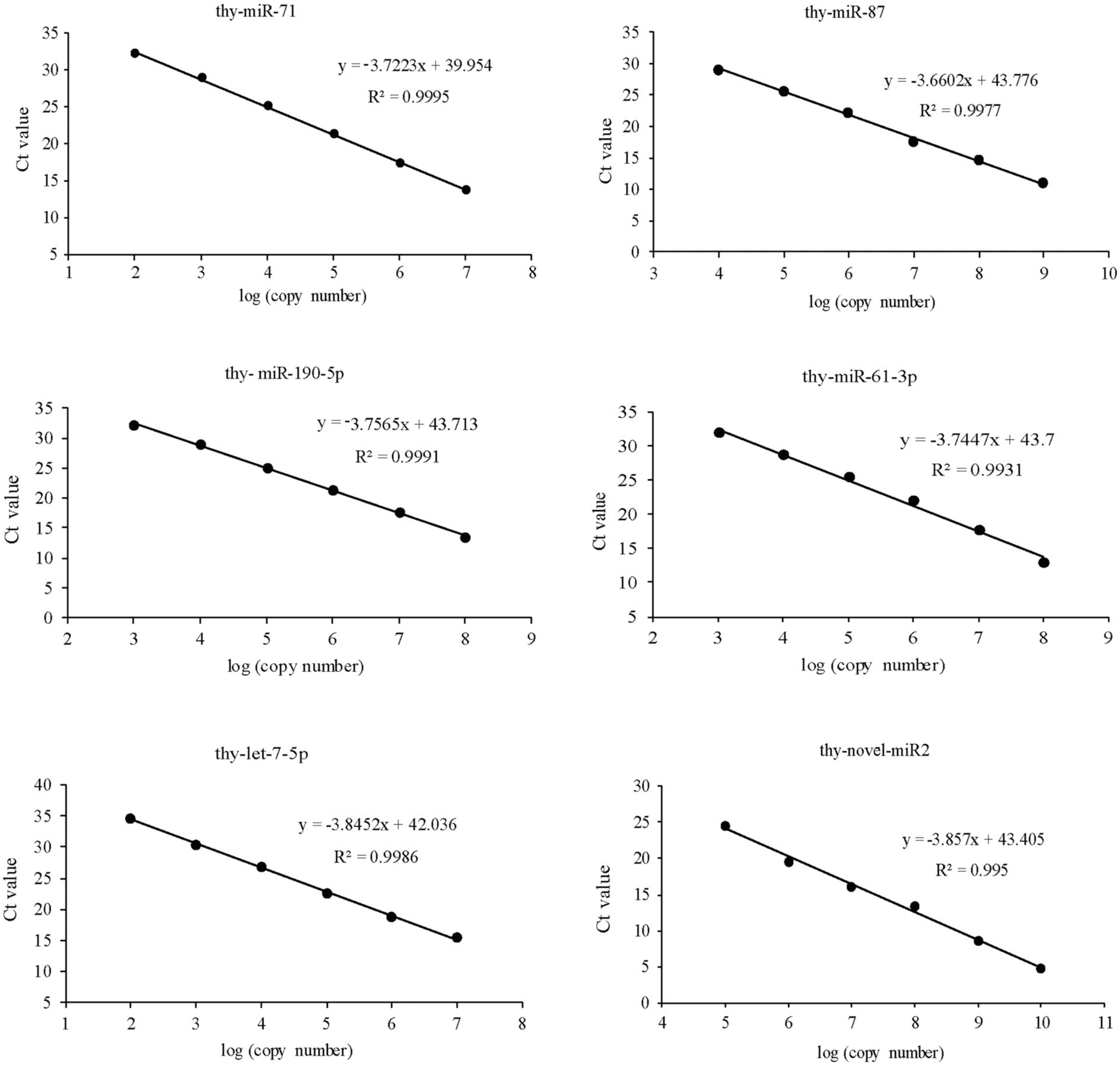

Fig. A3. Standard curves of 6 selected miRNAs.

References

Ai, L., Xu, M.J., Chen, M.X., Zhang, Y.N., Chen, S.H., Guo, J., Cai, Y.C., Zhou, X.N., Zhu, X.Q., Chen, J.X., 2012. Characterization of microRNAs in *Taenia saginata* of zoonotic significance by Solexa deep sequencing and bioinformatics analysis. Parasitol. Res. 110, 2373–2378.

Arora, N., Tripathi, S., Singh, A.K., Mondal, P., Mishra, A., Prasad, A., 2017. Micromanagement of immune system: role of miRNAs in helminthic infections. Front. Microbiol. 8, 586.

Bartel, D.P., 2004. MicroRNAs: genomics, biogenesis, mechanism, and function. Cell 116, 281–297.

Boulias, K., Horvitz, H.R., 2012. The *C. elegans* microRNA mir-71 acts in neurons to promote germline-mediated longevity through regulation of DAF-16/FOXO. Cell Metab. 15, 439–450.

Braae, U.C., Kabululu, M., Normark, M.E., Nejsum, P., Ngowi, H.A., Johansen, M.V., 2015. *Taenia hydatigena* cysticercosis in slaughtered pigs, goats, and sheep in Tanzania. Trop. Anim. Health Prod. 47, 1523–1530.

Cai, P., Gobert, G.N., You, H., Duke, M., McManus, D.P., 2015. Circulating miRNAs: potential novel biomarkers for Hepatopathology progression and diagnosis of *Schistosomiasis japonica* in two murine models. PLoS Negl. Trop. Dis. 9, e0003965.

Cai, P., Gobert, G.N., McManus, D.P., 2016. MicroRNAs in parasitic helminthiases: current status and future perspectives. Trends Parasitol. 32, 71–86.

Cucher, M., Macchiaroli, N., Kamenetzky, L., Maldonado, L., Brehm, K., Rosenzvit, M.C., 2015. High-throughput characterization of *Echinococcus spp*. metacestode miRNomes. Int. J. Parasitol. 45, 253–267.

Entwistle, L.J., Wilson, M.S., 2017. MicroRNA-mediated regulation of immune responses to intestinal helminth infections. Parasite Immunol. 39.

Formisano-Treziny, C., de San Feliciano, M., Gabert, J., 2012. Development of plasmid calibrators for absolute quantification of miRNAs by using real-time qPCR. J Mol Diagn 14, 314–321.

Friedlander, M.R., Chen, W., Adamidi, C., Maaskola, J., Einspanier, R., Knespel, S., Rajewsky, N., 2008. Discovering microRNAs from deep sequencing data using miRDeep. Nat. Biotechnol. 26, 407–415.

Guo, X., Zheng, Y., 2018. Identification and characterization of microRNAs in a cestode *Hydatigera taeniaeformis* using deep sequencing approach. Exp. Parasitol. 194, 32–37.

Guo, X., Zhang, X., Yang, J., Jin, X., Ding, J., Xiang, H., Ayaz, M., Luo, X., Zheng, Y., 2017. Suppression of nemo-like kinase by miR-71 in *Echinococcus multilocularis*. Exp. Parasitol. 183, 1–5.

Kang, C.W., Lim, H.G., Yang, J., Noh, M.H., Seo, S.W., Jung, G.Y., 2018. Synthetic auxotrophs for stable and tunable maintenance of plasmid copy number. Metab. Eng. 48, 121–128.

Li, R., Yu, C., Li, Y., Lam, T.W., Yiu, S.M., Kristiansen, K., Wang, J., 2009. SOAP2: an improved ultrafast tool for short read alignment. Bioinformatics 25, 1966–1967.

Luo, H., Zhang, H., Li, K., Rehman, M.U., Mehmood, K., Lan, Y., Huang, S., Li, J., 2017. Epidemiological survey and phylogenetic characterization of *Cysticercus tenuicollis* isolated from Tibetan pigs in Tibet, China. Biomed. Res. Int. 2017, 7857253.

Singh, B.B., Sharma, R., Gill, J.P., Sharma, J.K., 2015. Prevalence and morphological characterisation of *Cysticercus tenuicollis* (*Taenia hydatigena* cysts) in sheep and goat from North India. J. Parasit. Dis. 39, 80–84.

Sissay, M.M., Uggla, A., Waller, P.J., 2008. Prevalence and seasonal incidence of larval and adult cestode infections of sheep and goats in eastern Ethiopia. Trop. Anim.

Health Prod. 40, 387–394.

Whelan, J.A., Russell, N.B., Whelan, M.A., 2003. A method for the absolute quantification of cDNA using real-time PCR. J. Immunol. Methods 278, 261–269.

Wu, J., Ding, J., Yang, J., Guo, X., Zheng, Y., 2018. MicroRNA roles in the nuclear factor kappa B Signaling pathway in cancer. Front. Immunol. 9, 546.

Zheng, Y., 2017. High-throughput identification of miRNAs of *Taenia ovis*, a cestode threatening sheep industry. Infect. Genet. Evol. 51, 98–100.

Zheng, Y., Cai, X., Bradley, J.E., 2013. microRNAs in parasites and parasite infection. RNA Biol. 10, 371–379.

Zheng, Y., Guo, X., He, W., Shao, Z., Zhang, X., Yang, J., Shen, Y., Luo, X., Cao, J., 2016. Effects of *Echinococcus multilocularis* miR-71 mimics on murine macrophage RAW264.7 cells. Int. Immunopharmacol. 34, 259–262.